Optimization of pH sensing using silicon nanowire field effect transistors with HfO_2 as the sensing surface

2011 Nanotechnology 22 405501

(http://iopscience.iop.org/0957-4484/22/40/405501)

Nanotechnology **22** (2011) 405501 (6pp) doi:10.1088/0957-4484/22/40/405501

Optimization of pH sensing using silicon nanowire field effect transistors with HfO_2 as the sensing surface

Sufi Zafar, Christopher D'Emic, Ali Afzali, Benjamin Fletcher, Y Zhu and Tak Ning

IBM T J Watson Research Center, PO Box 218, Yorktown Heights, NY 10598, USA

Received 19 June 2011, in final form 16 August 2011
Published 12 September 2011
Online at stacks.iop.org/Nano/22/405501

Abstract

Silicon nanowire field effect transistor sensors with SiO_2/HfO_2 as the gate dielectric sensing surface are fabricated using a top down approach. These sensors are optimized for pH sensing with two key characteristics. First, the pH sensitivity is shown to be independent of buffer concentration. Second, the observed pH sensitivity is enhanced and is equal to the Nernst maximum sensitivity limit of 59 mV/pH with a corresponding subthreshold drain current change of ~650%/pH. These two enhanced pH sensing characteristics are attributed to the use of HfO_2 as the sensing surface and an optimized fabrication process compatible with silicon processing technology.

(Some figures in this article are in colour only in the electronic version)

1. Introduction

The pH value plays a critical role in numerous biochemical reactions and is of utmost importance in the study of life sciences [1–10]. For example, the activity of proteins [1, 5, 7], enzymes [2, 6], cellular organelles [3–5] and cells [8, 9] are drastically affected by minute changes in pH value. Also, the pharmacological effectiveness of drugs can be altered by changing the pH of their local environment [8, 10, 11]. Hence, the ability to monitor pH with high sensitivity and spatial resolution can help elucidate many physiological processes with applications in drug discovery and medical diagnostics. Also, pH sensing plays an important role in environmental [12] and food industry [13] related applications. Hence, accurate and fast sensing of pH is of great interest in various fields of study. There are many different types of pH sensors such as near infrared spectroscopy [14], nuclear magnetic resonance [15], fluorescent pH indicators [16] and ion-sensitive field effect transistors [17]. In recent years, silicon nanowire field effect transistor (FET) sensors have been investigated for the sensing of bio-molecules and ions including pH [18–23]. Due to their small size, the nanowire FET sensors offer two important advantages: fast response time and high sensitivity due to large surface to volume ratios.

Several studies have investigated pH sensing using silicon nanowire FET sensors [6, 18–23]. These studies have demonstrated pH sensing with varying sensitivity. However, none of these studies has investigated the effect of ionic concentration of the solution on pH measurement sensitivity. This is an important property of a pH sensor and ideally the pH sensitivity should be independent of the buffer concentration. In the present study, we demonstrate silicon nanowire (width = 6 nm, height = 26.5 nm) FET sensors optimized for pH sensing. The pH sensitivity is shown to be independent of the buffer concentration. Also, the observed pH sensitivity is equal to the Nernst maximum sensitivity limit of 59 mV/pH with a corresponding subthreshold drain current change of ~650%/pH. These pH sensing characteristics are shown to be consistent with the predictions of a previously proposed site binding model. In addition to the above stated key characteristics, these nanowire sensors show no measurable hysteresis or drifts and have low power requirements with a sensing voltage of ~0.5 V. These improvements are achieved by introducing a higher permittivity gate dielectric for the sensing surface and an improved top down fabrication process. A key feature of these sensors is the use of the bilayer SiO_2/HfO_2 as the gate dielectric stack where the HfO_2 layer is the sensing surface in contact with the buffer solution and SiO_2 forms the interfacial layer at the silicon channel. Using HfO_2 as the sensing surface has an important advantage over SiO_2: pH sensitivity is higher and is independent of the buffer concentration. The presence of a SiO_2

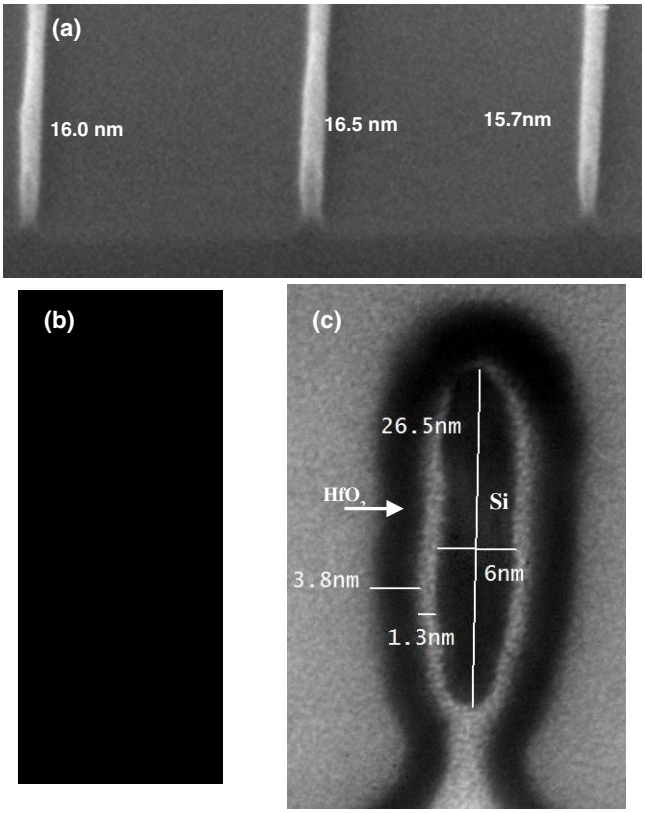

Figure 1. (a) Tilted angle SEM images of an array of nanowire FET sensors; the nanowire sensor width is ∼16 nm with 0.8 nm variation from sensor to sensor. (b) The top down SEM image of a nanowire sensor shows that there is no significant thinning or roughening along the length of the nanowire. (c) The cross-sectional TEM image of a nanowire FET sensor: the silicon nanowire (labeled as Si) is 6 nm wide and 26.5 nm high and has a SiO_2/HfO_2 stack covering the silicon wire; SiO_2 is 1.3 nm thick and the HfO_2 layer is 3.8 nm thick.

interfacial layer results in improved FET characteristics such as reduced subthreshold swing (∼77 mV/decade) and absence of hysteresis. Improvements in the fabrication processes are also introduced in order to minimize the fabrication related damage to the silicon nanowire surface. Lastly, the nanowire FET sensors are fabricated using only those processes and materials that are compatible with silicon processing technology, and can therefore be cost effectively integrated with circuitry for automation and multiplexing.

2. Fabrication of silicon nanowire FET sensors

In this study, the FET based sensor consists of a lightly doped silicon nanowire channel, heavily boron doped source and drain regions, SiO_2/HfO_2 bilayer as the gate dielectric sensing surface and the buffer solution as the gate. These FET sensors are fabricated using standard silicon processing technology [24]. The main fabrication steps are as follows. The starting material is commercially available eight inch silicon-on-insulator (SOI) wafers with lightly doped ($\sim 10^{15}$ cm^{-3}) p-type silicon, 145 nm thick buried oxide (BOX) thickness and 55 nm thick top silicon layer. First, the top silicon layer was reduced to ∼30 nm thickness by thermal oxidation and wet etching processes; oxidation is performed at 900 °C in oxygen and wet etching is done using dilute (1%) hydrofluoric acid. Second, the thinned blanket silicon layer is patterned into silicon nanowires (width ∼ 10 nm, height = 30 nm, length = 5 μm), leads (1 mm long) and bond pads (80 × 80 μm^2) using electron beam lithography and reactive ion etch (RIE) processing [25–27]. In contrast to the wet etching process [20], the RIE is an anisotropic etch that provides superior profile control with less breakage and thinning of wires. Hence, RIE is more suitable for forming nanowires of narrow width. However, RIE causes damage to the active silicon layer which degrades sensor sensitivity [20, 28, 29]. In order to resolve this issue, the damaged silicon layer (∼2.5 nm) is removed from the nanowire surface by first thermally oxidizing the damaged silicon and then removing the oxidized surface by using a dilute (1%) hydrofluoric acid etching process. The third fabrication step involves the deposition of a SiO_2/HfO_2 gate dielectric bilayer over the silicon nanowire. The SiO_2 layer of 1.5 nm thickness is formed by the rapid thermal oxidation at 900 °C of the silicon nanowire surface. Once the high temperature thermal SiO_2 layer is formed, 4 nm thick HfO_2 is deposited by chemical vapor deposition (CVD) at 500 °C [30]. In this work, HfO_2 is selected as the sensing surface because it not only has excellent pH sensing properties but is also chemically inert in most acidic and basic solutions with the exception of hydrofluoric acid (HF) based solutions [31]. Our studies show that the dilute (1%) HF aqueous solution etches HfO_2 at the rate of <2 Å min^{-1}. In addition, thin HfO_2 films have been extensively investigated as the gate dielectric in advanced FET applications [31–35], and consequently extensive literature on these films is available which can be utilized for the development of sensor applications. Previous studies on HfO_2 gate dielectric applications have shown that the deposition of a HfO_2 layer directly on silicon results in degradation of device characteristics due to increased charge trapping, hysteresis and subthreshold swing; these degradations can be reduced by forming a SiO_2 interfacial layer [32–35]. Hence, a bilayer of SiO_2/HfO_2 is used as the gate dielectric in the FET sensors. The fourth fabrication step consists of the implantation and activation of boron in the source and drain regions, leads and bond pads. The dopant activation is achieved by performing a rapid thermal anneal at 1000 °C for 5 s in a nitrogen ambient. The fifth step is the formation of a NiPt silicide layer over the source and drain regions, leads and bond pads by sputter deposition of Ni (5% Pt) followed by 400 °C rapid thermal anneal in a nitrogen ambient. The final fabrication step involves the deposition of 1000 Å thick ozone tetra-ethyl orthosilicate (TEOS) oxide at 400 °C that covers the source/drain regions and the leads whilst keeping the nanowires and bond pads exposed. Figure 1 shows the scanning electron microscopy (SEM) and transmission electron microscopy (TEM) images of fabricated silicon nanowire FET sensors. Figure 1(a) is the tilted angle, top down SEM image of nanowire FET sensors. From this image, we observe the sensor width to be about 16 with 0.8 nm variation from sensor to sensor. Figure 1(b) is a top down SEM image showing that the

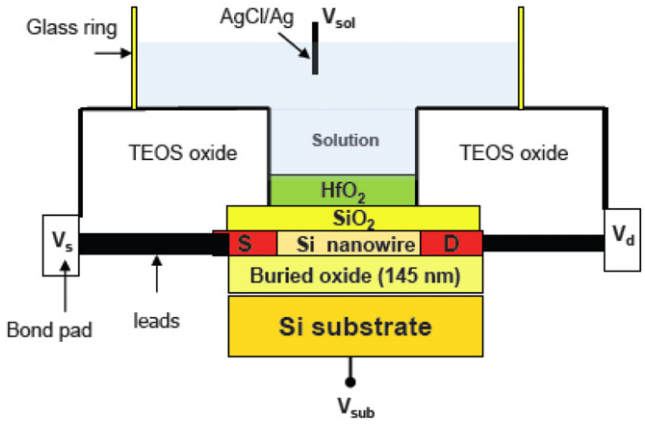

Figure 2. Schematics for pH sensing using a nanowire FET based sensor. Silicon nanowire forms the channel (width = 6 nm, height = 26.5 nm, length = 5 μm) and HfO_2 is the sensing surface and the buffer solution functions as the gate. S and D denote source and drain regions, respectively; BOX is the buried oxide. Source and drain regions and the leads to the bond pads are covered with 1000 Å thick TEOS oxide and only the HfO_2 sensing surface is exposed to the solution. A glass ring (1 mm radius) glued to the TEOS oxide surface forms the chamber for holding the solution under study. V_s, V_d and V_{sub} are the voltages applied at the source, drain and silicon substrate, respectively. V_{sol} is the voltage applied to the AgCl/Ag electrode immersed in the phosphate buffer solution.

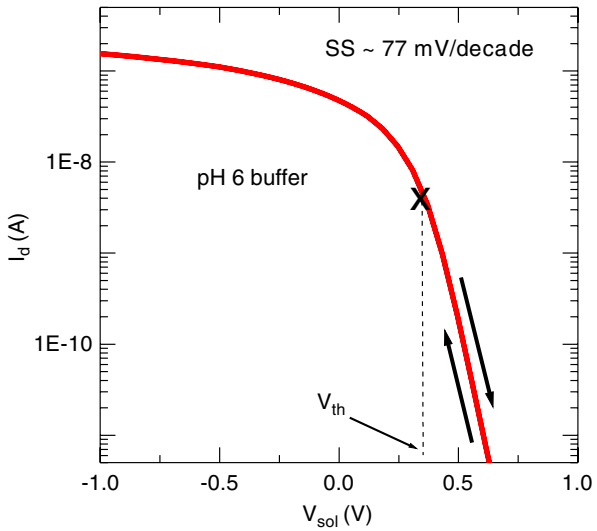

Figure 3. Dependence of the measured drain current (I_d) on the gate voltage (V_{sol}) at room temperature; V_{sol} is applied to the phosphate buffer solution which forms the gate; the gate voltage is double swept from 0.6 to −1 V as indicated by the arrows in steps of 50 mV. SS is the subthreshold swing and V_{th} is the threshold voltage; I_d varies exponentially in the subthreshold regime where $V_{sol} > V_{th}$.

fabricated nanowire is uniformly thick along its length with no indication of thinning. Figure 1(c) shows the cross-sectional TEM image of a nanowire FET. From the TEM image, we observe that the silicon nanowire is 6 nm wide and 26.5 nm high with SiO_2/HfO_2 as the gate dielectric stack; SiO_2 forms an interfacial layer of 1.3 nm thick and the HfO_2 layer has a conformal coverage of 3.8 nm thickness.

3. pH sensing results and discussion

Once the nanowire FET sensors were fabricated, a glass ring (∼1 mm radius) was bonded to the TEOS surface to form a chamber for holding the solution under investigation. Figure 2 shows the schematics for performing pH sensing measurements using nanowire FET sensors. The buffer solution is used as the gate and the gate voltage (V_{sol}) is applied to the Ag/AgCl electrode immersed in the solution. The sensing signal is the drain current which is measured as a function of gate voltage (V_{sol}) whilst holding the drain voltage (V_d), source voltage (V_s) and substrate voltage (V_{sub}) constant; $V_d = -50$ mV, $V_s = V_{sub} = 0$ V. All the measurements in this study are performed at room temperature using the above stated voltage settings and phosphate buffer solution (Sigma Aldrich Co.) of varying pH values unless otherwise stated.

Before performing pH sensing measurements, the fabricated nanowire FET sensors are evaluated for fabrication induced degradation of sensor characteristics such as subthreshold swing and hysteresis. Both these characteristics degrade mainly due to the presence of interfacial defects that are created during the fabrication processes such as reactive ion etching (RIE) and HfO_2 deposition. The subthreshold swing is defined as the gate voltage required for varying the subthreshold drain current by a decade. Hence, smaller subthreshold swing values are desirable as smaller values would result in higher sensitivity. Hysteresis occurs due to defects at the silicon channel interface and causes the sensing measurements to be irreproducible. Figure 3 shows the dependence of the drain current (I_d) on the gate voltage (V_{sol}) applied to the phosphate buffer solution of pH 6. V_{sol} is varied from 0.8 to −1.0 V and back to 0.8 V in a double sweep as indicated by the two arrows. The threshold voltage (V_{th}) is 0.36 V as indicated in the figure. I_d has an exponential dependence on the gate voltage (V_{sol}) in the subthreshold regime ($V_{sol} > V_{th}$) and the subthreshold swing (SS) is equal to 77 mV/decade. This SS value is significantly smaller than the previously reported values of ∼180–500 mV/decade [20, 21]. The I_d–V_{sol} curve shows no hysteresis and is identical as the gate voltage is swept up and down. Since degradation in both the subthreshold swing and hysteresis arise due to defects at the silicon/SiO_2 interface [36], the observed small value of subthreshold swing and the absence of hysteresis indicate that these nanowire FET sensors have reduced defect density at the Si/SiO_2 interface. Hence, interfacial defect creation has been successfully minimized in the fabrication of silicon nanowire FET sensors. In addition, drifts in the drain currents were monitored over several hours (∼10 h) with no measurable shifts.

Figure 4 shows the pH sensing results for the silicon nanowire FET sensor with HfO_2 as the sensing surface. The measurements are performed using 100 mM concentration of phosphate buffer solutions of varying pH values (10–4). Figure 4(a) shows the measured dependence of the drain current (I_d) on the gate voltage (V_{sol}) for various pH values. The I_d–V_{sol} curve is observed to shift toward higher gate voltage while the subthreshold swing remains unchanged as the pH value increases. From figure 4(a), we observe that the

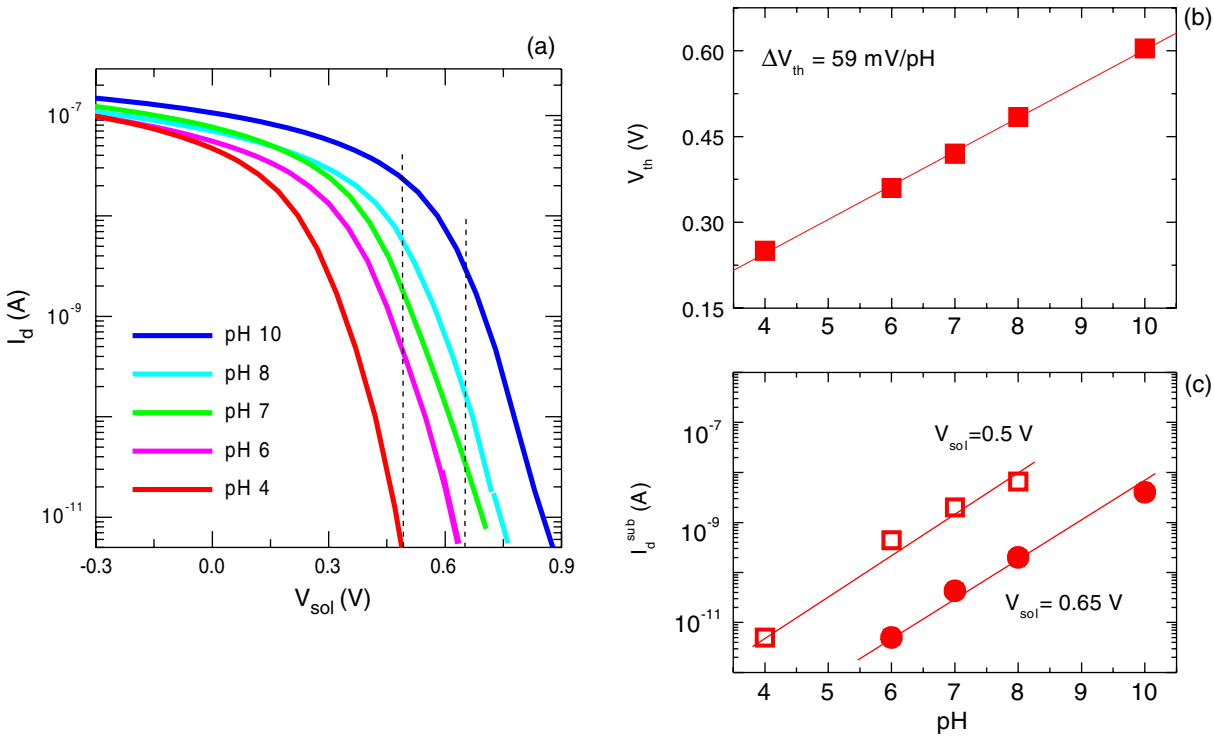

Figure 4. (a) The drain current (I_d) versus gate voltage (V_{sol}) curves measured at room temperature and varying pH values of the phosphate buffer of 100 mM concentration; the two vertical dashed lines indicate V_{sol} values of 0.5 and 0.65 V. (b) Dependence of the threshold voltage (V_{th}) on pH values; the symbols are the measured V_{th} obtained from (a) and the solid line is the linear fit with a slope of 59 mV/pH. (c) Dependence of the subthreshold drain current (I_d^{sub}) on pH values; drain current data are extracted at V_{sol} of 0.5 and 0.65 V from (a); I_d^{sub} at 0.5 V corresponding to pH 10 is outside the subthreshold regime as can be seen from (a) and is therefore omitted. Symbols are the measured drain currents and solid lines are exponential fits: $I_d^{sub} \propto \exp^{m\text{pH}}$ with $m = 2.01$. From the exponential fits, subthreshold drain current change $\Delta I_d^{sub}/I_d^{sub}$ is estimated to be about 650%/pH.

sensing signal I_d shows the largest variation with pH in the subthreshold regime. For example, the subthreshold regime I_d at $V_{sol} = 0.65$ V increases by about 1000 times as the pH increases from 6 to 10. In comparison, the linear regime I_d at $V_{sol} = -0.3$ V increases by only twice over the same pH range. Hence, maximum sensitivity would be observed when the sensing signal I_d is measured in the subthreshold regime, consistent with the conclusion of a previous study [22]. In order to further examine the pH sensitivity, threshold voltages and subthreshold drain currents are extracted from figure 4(a) and their dependence on pH is analyzed. Figure 4(b) shows that the threshold voltage (V_{th}) varies linearly with pH with a shift of $\Delta V_{th} = 59$ mV/pH. This shift is equal to the Nernst sensitivity limit of $\Delta V_{th} = 59.2$ mV/pH at room temperature [38]. Hence, the HfO_2 surface shows maximum pH sensitivity without requiring any surface modification, and is about two times higher than those for more widely used SiO_2 surfaces with ΔV_{th} in the range of 30–40 mV/pH [22, 38, 39]. This ΔV_{th} sensitivity depends predominantly on the intrinsic properties of the sensing surface [38, 39] and has only a weak dependence on the fabrication process. In other words, the HfO_2 sensing surface has superior sensitivity to pH in comparison to SiO_2 surfaces. As discussed earlier, the drain current shows the largest dependence on the gate voltage in the subthreshold regime and therefore the dependence of the subthreshold drain current (I_d^{sub}) on pH is investigated, as shown in figure 4(c). In figure 4(c), I_d^{sub} at $V_{sol} = 0.5$ and 0.65 V are plotted as a function of pH. I_d^{sub} is observed to increase exponentially with increasing pH for both the plots corresponding to $V_{sol} = 0.5$ and 0.65 V. From the exponential fits, the subthreshold drain current dependence on pH can be written as: $I_d^{sub} \propto \exp^{m\text{pH}}$ with $m = 2.01$. Hence from the fits, I_d^{sub} increases by ~7.5 times as pH is increased by a unit and $\Delta I_d^{sub}/I_d^{sub} \sim 650\%$/pH. The observed high pH sensitivity is attributed to combined contributions of HfO_2 as the sensing surface, the miniaturization process and an improved fabrication process. Lastly from figure 4(b), the measured threshold voltage values are observed to be low ($|V_{th}| < 1.0$ V) which implies that the sensing voltage would also be less than 1.0 V. These low threshold voltage values are attributed mainly to two factors: (i) reduced fixed charge density in the SiO_2/HfO_2 gate stack and (ii) use of electrolyte as the top gate for sensing measurements, as shown in figure 2. The creation of fixed charge density in the SiO_2/HfO_2 stack is minimized by controlling process related damage and contamination during the fabrication process. In the top gate configuration, the SiO_2/HfO_2 stack forms the gate dielectric and has an equivalent oxide thickness (EOT) of about 3.1 nm. This EOT value is significantly smaller than the thicker (145 nm) BOX thickness which would form the gate dielectric layer if the sensing measurements were performed with the silicon substrate as the back gate. Since the threshold voltage depends on the gate

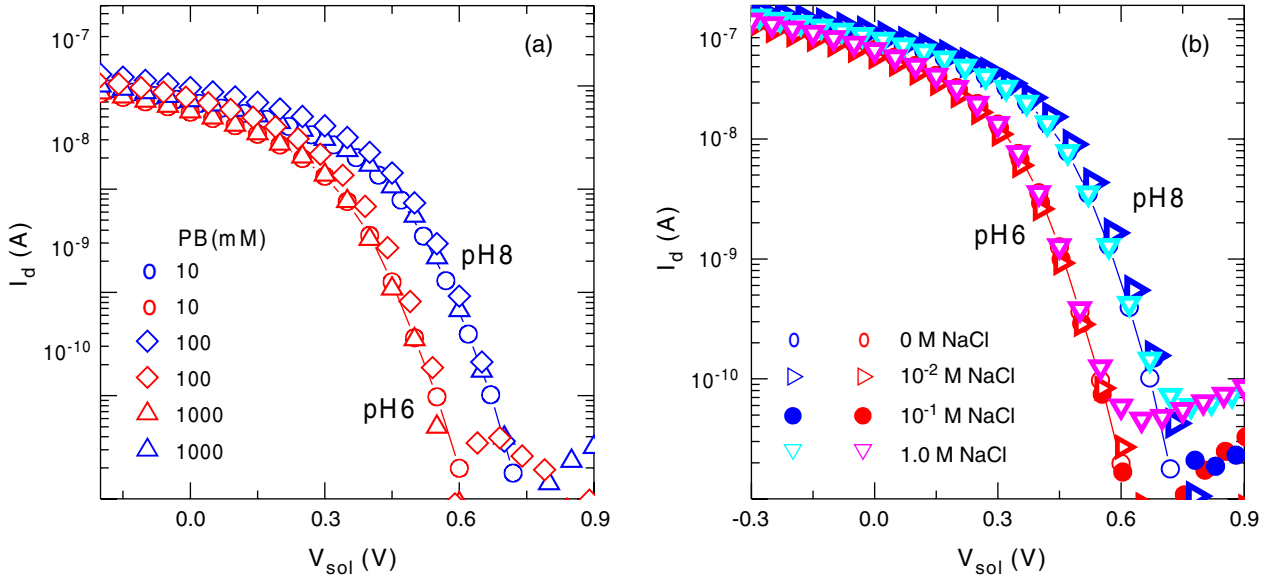

Figure 5. Dependence of measured I_d–V_{sol} curves on the ionic concentrations of the phosphate buffer (PB) solutions at pH 6 and pH 8. (b) Dependence of I_d–V_{sol} curves on NaCl concentrations in 10 mM phosphate buffer solution at pH 6 and pH 8.

dielectric EOT [36], sensing measurements performed with the buffer solution as the top gate result in smaller threshold values, as observed in figure 4(b). In summary, highly miniaturized silicon nanowire FET sensors with high pH sensitivity and low sensing voltage requirements are demonstrated.

An important attribute of a pH sensor is the requirement that the pH sensitivity be independent of the buffer concentration. In figure 5(a), I_d–V_{sol} curves are measured at pH 6 and 8 of phosphate buffer solutions of varying concentrations (10, 100 and 1000 mM). As shown in the figure, the drain current versus gate current curve depends only on the pH value and is independent of the buffer concentration. The I_d–V_{sol} curve is observed to shift by about 59 mV/pH with a corresponding $\Delta I_d^{sub}/I_d^{sub} \sim 650\%$/pH, irrespective of the buffer concentration. Hence, phosphate buffer concentration has negligible influence on the pH sensitivity of the HfO_2 sensing surface. In order to further verify this property, pH sensing is performed in 10 mM of the phosphate buffer solution at pH 8 and 6 with varying NaCl concentrations of 0, 0.01, 0.1 and 1 M. Once again, the pH sensitivity is independent of NaCl concentration, as shown in figure 5(b). In comparison, the more widely used SiO_2 sensing surface does not exhibit this desirable pH sensing property [37, 38].

The observed pH sensing properties of HfO_2 as shown in figures 4 and 5 can be understood by a previously proposed model [38, 39]. According to the model, the pH sensitivity of the sensing surface arises from the interactions of protons with the surface. The surface is assumed to have specific sites that can bind protons from the solution, thus giving rise to pH dependent surface charge density. As a result of this pH dependent surface charge density, an equal but opposite sign of the diffused layer of charges is created in the solution. These two charge layers form a double layer capacitance with ψ_o as the electrostatic potential difference across the double layer. In summary, binding of protons to the HfO_2 surface results in the formation of a dipole layer at the solid/liquid interface, thus causing the surface charge density and the concomitant electrostatic potential difference ψ_o to change with the pH of the solution. Hence, the pH sensitivity can be defined as:

$$\delta\psi_o/\delta\mathrm{pH} = -2.3kTq^{-1}\alpha$$
$$\alpha = \{(2.3kTC_{dif}q^{-2}\beta_{int}^{-1}) + 1\}^{-1} \quad (1)$$

where T is the temperature in Kelvin, q is the magnitude of an electronic charge, k is the Boltzmann constant, α is a dimensionless sensitivity parameter, β_{int} is the intrinsic buffer capacity and C_{dif} is the differential capacitance. The β_{int} value depends on the sensing surface characteristics such as binding site density and binding energies for protons. The C_{dif} value depends on the concentration and charge of each ion type in the solution. From equation (1), we observe that when $\beta_{int} \gg C_{dif}$ then $\alpha = 1$. This implies that the predicted pH sensitivity would have a maximum value of 59.2 mV/pH at room temperature and that the sensitivity would be independent of ionic concentration of the solution. These two predictions are in agreement with the pH sensing results observed for HfO_2, as shown in figures 4(b) and 5.

4. Conclusions

FET sensors with a silicon nanowire (width = 6 nm, height = 26.5 nm) channel and SiO_2/HfO_2 gate dielectric sensing surface are fabricated using a top down fabrication approach compatible with silicon processing technology. The nanowire FET sensors are demonstrated to exhibit pH sensitivity that is independent of the ionic concentrations in the solution. Moreover, the observed pH sensitivity is observed to be the Nernstian maximum limit of $\Delta V_{th} = 59$ mV/pH at room temperature with a corresponding subthreshold drain current change of 650%/pH. These two pH sensing characteristics

are shown to be consistent with a previously proposed site binding model. Also, the sensing voltage is low (<|1| V) and the drain current versus gate voltage curves show no measurable hysteresis or drifts with time. Hence, these silicon nanowire FET sensors are optimized for pH sensing. Lastly, the pH sensitivity is often used to benchmark FET based sensor characteristics. The fabrication optimization results (e.g. reduced subthreshold swing of 77 mV/decade and low threshold voltage (<|1.0| V)) presented in this study would also be applicable for label free detection of bio-molecules using similar sensors.

Acknowledgments

We would like to thank J Stathis, D Park, G Shahidi and T C Chen for their encouragement and management support for the project. We would also like to thank M Guillorn for his suggestions and comments.

References

[1] Yang A-S and Honig B 1993 *J. Mol. Biol.* **231** 459–74
[2] Chance B 1952 *J. Biol. Chem.* **194** 471–81
[3] Roos A and Boron W F 1981 *Physiol. Rev.* **61** 296–434
[4] Kamp F, Donoso P and Hidalgo C 1998 *Biophys. J.* **74** 290–6
[5] Nakamura N, Tanaka S, Teko Y, Mitsui K and Kanazawa K 2004 *J. Biol. Chem.* **280** 1561–72
[6] Chen Y, Wang X, Hong M, Erramilli S and Mohanty P 2008 *Sensors Actuators* B **133** 593–8
[7] Kummer U *et al* 2007 *Biophys. J.* **92** 2597–607
[8] Li X J and Schick M 2001 *Biophys. J.* **80** 1703–11
[9] Lipton P 1999 *Physiol. Rev.* **79** 1431–568
[10] Borges R, Travis E R, Ochstetler S E and Lightman R M 1997 *J. Biol. Chem.* **272** 8325–31
[11] Katsura K, Asplund B, Ekholm A and Siesjo B K 1992 *Eur. J. Neurosci.* **4** 166–76
[12] Frost R R and Griffin R A 1977 *Soil Sci. Soc. Am. J.* **41** 1–5
[13] Royce P N 1993 *Crit. Rev. Biotechnol.* **13** 117–49
[14] Soyemi O, Shear M and Landry M 2005 *Proc. SPIE* **6007** 60070N
[15] Yoshioka Y *et al* 2002 *Spectroscopy* **16** 183–90
[16] Leiner M J P and Wolfbeis O S 2007 *Fiber Optic Chemical Sensors and Biosensors* (Boca Raton, FL: CRC Press) pp 359–84
[17] Bergveld P 2003 *Sensors Actuators* B **88** 1–20
[18] Cui Y, Wei Q, Park H and Lieber C M 2001 *Science* **293** 1289–92
[19] Zheng G, Patolsky F, Cui Y, Wang W and Lieber C 2005 *Nature Biotechnol.* **23** 1294–301
[20] Stern E, Klemic J F, Routenberg D A, Wyrembak P N, Turner-Evans D B, Hamilton A D, LaVan D A, Fahmy T M and Reed M A 2007 *Nature* **445** 519–22
[21] Knopfmacher O, Tarasov A, Fu W, Wipf M, Niesen B, Calame M and Schonenberger C 2010 *Nano Lett.* **10** 2268–74
[22] Gao X A, Zheng G and Lieber C 2010 *Nano Lett.* **10** 547–52
[23] Chen S, Bomer J, Carlen E T and Berg A 2011 *Nano Lett.* **8** 2334–40
[24] Wolf S and Tauber R N 2000 *Silicon Processing for the VLSI Era-Process Technology* vol 1 (Sunset Beach, CA: Lattice Press) pp 149–838
[25] Guillorn M *et al* 2009 *J. Vac. Sci. Technol.* B **27** 2588–92
[26] Glodde M *et al* 2011 *Proc. SPIE* **7972** 797216
[27] Gunawan O, Sekaric L, Majumdar A, Rooks M, Appenzeller J, Sleight J, Guha S and Haensch W 2008 *Nano Lett.* **8** 1566–71
[28] Cheng M M-C *et al* 2006 *Curr. Opin. Chem. Biol.* **10** 11–9
[29] Li Z *et al* 2004 *Nano Lett.* **4** 245–7
[30] Callegari A *et al* 2006 *US Patent Specification* 7566938
[31] Shamiryan D, Baklanov M, Claes M, Boullart W and Paraschib V 2009 *Chem. Eng. Commun.* **196** 1475–535 Robertson J 2006 *Rep. Prog. Phys.* **69** 327–39
[32] Zafar S, Kumar A, Gusev E and Cartier E 2005 *IEEE Trans. Device Mater. Reliab.* **5** 45–64
[33] Zhu W.J, Ma T P, Zafar S and Tamagawa T 2002 *Electron. Device Lett.* **23** 597–9
[34] Gusev E P *et al* 2001 *IEDM Technical Digest* 2001 pp 20.1.1–4
[35] Stesmans A and Afanasev V V 2003 *Appl. Phys. Lett.* **82** 4074–6
[36] Hori T 1997 *Gate Dielectrics and MOS ULSI* (Berlin: Springer) pp 80–90
[37] Bolt G H 1957 *J. Phys. Chem.* **61** 1166–9
[38] Hal R E G, van Eijkel J C T and Bergveld P 1995 *Sensors Actuators* B **24/25** 201–5
[39] Bergveld P 1996 *Sensors Actuators* A **56** 65–73